Journal of the Meteorological Society of Japan

EARLY ONLINE RELEASE

The DOI for this manuscript is
DOI:10.2151/jmsj.2023-016
J-STAGE Advance published date: March 24th, 2023

Interannual Variability of Dust Deposition in Japan during Spring Season and Related Atmospheric Circulation Fields

Masaya KURAMOCHI[1]

Graduate School of Science and Technology, University of Tsukuba, Tsukuba, Ibaraki, Japan.

Meteorological Research Institute (MRI), Japan Meteorological Agency (JMA), Tsukuba, Ibaraki, Japan.

Mizuo KAJINO

Meteorological Research Institute (MRI), Japan Meteorological Agency (JMA), Tsukuba, Ibaraki, Japan.

Faculty of Life and Environmental Sciences, University of Tsukuba, Tsukuba, Ibaraki, Japan.

and

Hiroaki UEDA

Faculty of Life and Environmental Sciences, University of Tsukuba, Tsukuba, Ibaraki, Japan.

August 25, 2022

December 22, 2022

February 7, 2023

----

1) Corresponding author: Masaya Kuramochi, Graduate School of Science and Technology, University of Tsukuba, 1-1-1 Tennodai, Tsukuba, Ibaraki, 305-8572 JAPAN

Email: kuramochi.masaya.sp@alumni.tsukuba.ac.jp

Tel: +81-29-853-5692

Abstract

Mineral dust affects health, climate, and ecosystems in various ways. East Asia is one of the major sources of mineral dust in the world. This study examines the year-to-year variability of dust deposition over Japan in April from the perspective of large-scale atmospheric circulations using atmospheric and aerosol reanalysis datasets for the period from 2011 to 2017. The increased dust deposition in Japan is explained by the intensified dust transport from the Mongolian Plateau by the anomalous westerly winds associated with a deepened trough over the East Asian continent toward the northwest of the Japanese islands in the middle to lower troposphere. The enhanced dust emission over Gobi Desert and the intensified extratropical cyclone activity are consistent with the larger-than-normal amount of dust in East Asia. Comparing the dust depositions over western and northern Japan, it is suggested that the slightly different anomalous trough positions may determine whether or not a large amount of dust is carried. A further analysis using the long-term (1967–2022) observation data of dust in Japan supports the importance of the intensified trough over the East Asian continent. Dust flux decomposed into cyclonic and anticyclonic components showed that both vortices contribute to the eastward dust transport in East Asia. These results suggest that Japanese dust events and their variability are affected by the stationary circulation anomaly as well as the baroclinic instability waves including transient cyclones and anticyclones.

Keywords mineral dust; aerosol; dust transport; interannual variability

1. Introduction

Mineral dust particles affect health, climate, and ecosystems in various ways. These particles in surface air are detrimental to human health (Perez et al. 2008; Stafoggia et al. 2016; Hashizume et al. 2020). Dust promotes the chemical formation of toxic substances, such as nitropolycyclic aromatic hydrocarbons, on its particle surfaces (Kameda et al. 2016). It affects regional climate via the aerosol–radiation (both shortwave and longwave) and aerosol–cloud interactions by acting as both cloud condensation nuclei and ice-nucleating particles (Szopa et al. 2021). Once deposited to the ground surface, it supplies nutrients for marine and terrestrial plants (Ridgwell 2002; Zhang et al. 2018) and reduces the risk of acid deposition due to its neutralization effect (Terada et al. 2002; Rastogi and Sarin 2006). Dust deposition on snow and ice surfaces promotes their melting (Di Mauro et al. 2019; Niwano et al. 2021).

East Asia is one of the major source regions of mineral dust in the world (Tanaka and Chiba 2006; Hu et al. 2019) and it originates from the Mongolian Plateau (mainly Gobi and Taklimakan Deserts). Because dust cannot be emitted under the weak surface winds, snow cover during winter, and vegetation during summer, East Asian dust events more frequently occur in April when the plateau land surface is open and strong surface winds frequently occur (Littmann 1991; Parungo et al. 1994; Kurosaki and Mikami 2003, 2004, 2005). Moreover, the Asian monsoon starts to turn from the winter phase to the summer phase in April, which is characterized by the turnabout of wind direction and northward extension of the precipitation zone (Qian et al. 2002a; Ueda 2005; Ueda et al. 2009). A developing extratropical cyclone and associated cold front are identified as important factors for dust emission in Gobi Desert (Kawai et al. 2015, 2018). Emitted dust from Gobi Desert is transported to Korea and Japan by middle- to lower-tropospheric winds (Iwasaka et al. 1983; Parungo et al. 1994; Onishi et al. 2012). Taklimakan Desert is also a major source of mineral dust in East Asia (Uno et al. 2009; Yumimoto et al. 2019). Unlike Gobi, Taklimakan dust is mainly transported to the free troposphere (Matsuki et al. 2003) and around the Northern Hemisphere (Uno et al. 2009) because the Tarim basin is surrounded by high mountains with elevations of more than 5000 m. Dust containing air mass is forced to ascent before being transported out of the basin (Sun et al. 2001; Tsunematsu et al. 2005).

As for the interannual variability, the dust storm frequency over East Asia is closely related to the modulation of a large-scale atmospheric circulation (Qian et al. 2002b; Gong et al. 2006a; Gong et al. 2006b; Kim 2008; Yang et al. 2008; Han et al. 2008). Qian et al. (2002b) showed that the increased cyclone frequency associated with the anomalous air temperature gradient is responsible for the high dust storm frequency in China. Kim (2008) pointed out that the geopotential height anomaly at the lower troposphere contributed to the intensified dust transport to southern Korea. The westerly jet variability accompanied by the anticyclonic circulation anomaly over the Mongolian Plateau and Middle Siberia is identified as an important factor in the long-term decreasing trend of dust storms over Taklimakan, Gobi Deserts, and the Tibetan Plateau since the 1970s or mid-1980s (Ding et al. 2005; Wang et al. 2008; Kang et al. 2016). Moreover, dust emission over northern China is strongly controlled by the land surface conditions such as soil moisture associated with precipitation anomaly as well as vegetation (Liu et al. 2004).

In Japan, although dust events and characteristics in the western side of Japan have been investigated (Zhang et al. 2003; Shimizu et al. 2004; Onishi et al. 2012), those of northern Japan have never been much examined. The impacts of dust deposition on the western and northern parts of Japan are distinct. Northern Japan, especially on the Sea of Japan side, is a heavy snowfall area (Ninomiya 1968; Steenburgh and Nakai 2020); hence, the impact of dust deposition on the surface snow is expected. The interannual variability of dust events has been reported, but the relationship between the interannual variability and the atmospheric circulations has not yet been assessed. This study investigates the characteristic of the anomalous atmospheric circulation associated with the interannual variation of dust deposition in western and northern Japan using an aerosol reanalysis dataset. Moreover, we attempt to reveal the climatological mean dust behavior and the continuous spatial distribution in the troposphere using three-dimensional (3D) dust concentration data.

2. Data and methods

2.1 Reanalysis datasets

The atmospheric data used were the Japanese 55-year Reanalysis dataset (JRA-55;

Kobayashi et al. 2015), with a horizontal resolution of 1.25° × 1.25° and 37 vertical levels from 1000 to 1 hPa, which is available from 1958. The global dust data were obtained from the Japanese Reanalysis for Aerosol (JRAero; Yumimoto et al. 2017) with a horizontal resolution of approximately 1.1° × 1.1°, 48 vertical levels using the hybrid sigma pressure coordinate system, and available from 2011 to 2017. JRAero employs a global aerosol transport model developed by the Meteorological Research Institute (MASINGAR mk-2; Yukimoto et al. 2012), which includes advection, convective, diffusive transport, emissions, chemical reaction, and removal processes. Satellite aerosol observations are assimilated by a two-dimensional variational data assimilation system (Yumimoto et al. 2017). It has been confirmed that the model simulation in MASINGAR (Tanaka et al. 2003) well reproduced the observed temporal variability of dust deposition in Japan (Tanaka and Chiba 2005; Lee et al. 2006; Inomata et al. 2009). In this study, the 3D variables in JRAero were vertically interpolated in 11 pressure levels from 1000 to 100 hPa to match with the JRA-55 pressure levels. The 6-hourly and monthly mean data of these reanalysis datasets from 2011 to 2017 were utilized considering the available period of JRAero. We additionally used dust observation data by the Japan Meteorological Agency (JMA) from 1967 to 2022. JMA has visually observed the carried dust at 11 stations in Japan and provides the number of dust observed days on their website (see Data Availability Statement).

2.2 Variations of dust deposition in Japan

A linear regression analysis between the interannual variations of dust deposition over Japan and the monthly mean atmospheric circulation fields was conducted. The dust deposition indices used for the regression analysis are defined as the area-averaged total dust deposition (i.e., dry plus wet deposition) of JRAero on land over the southwestern part [30–37°N, 129–137°E] (Domain 1) and the northeastern part of Japan [37–46°N, 137–146°E] (Domain 2) (color rectangles in Fig. 1a). The dust deposition on the sea was masked before the area average. As shown in Fig. 1b, the amount of deposited dust both in Domains 1 and 2 is maximized in April, which is consistent with the dust seasonality shown by previous studies. Thus, we focus on the April variability in this study. Figure 1a illustrates the amount of total dust deposition in April averaged in the whole analysis period. A large amount of dust deposits in western Japan, especially on the Sea of Japan side; however, the northern Japan deposition is almost the same amount, indicating the importance of dust analysis over northern Japan. Figure 1c depicts the mean dust deposition over Domains 1 and 2 for every analysis year. We may notice a striking interannual variability of dust deposition. The relationship of the magnitude of Domains 1 and 2 deposition amounts varied from year to year. In the following, the unit of regressed quantities was per one standard deviation (σ) of each index. 1σ of Domain 1 was 9.88 mg m^{-2} day^{-1} whereas that of Domain 2 was 13.08 mg m^{-2} day^{-1}. Statistical significance was confirmed through a *t*-test. For our analysis period, the statistically significant correlation coefficient at the 90% confidence level was approximately 0.67.

2.3 Dust flux and curvature

One of the goals of this study is to assess the separate contribution of cyclonic and anticyclonic winds to dust transport. In diagnosing the dust transport by wind, the horizontal dust flux $\mathbf{DF}$ is defined as follows:

$$\mathbf{DF} \equiv C_{\mathrm{dust}} \cdot \mathbf{v}, \qquad (1)$$

where C_{dust} is the dust concentration (μg m^{-3}) and $\mathbf{v} = (u, v)$ is the horizontal wind vector, with u as the zonal wind and v as the meridional wind. The time-averaged dust flux may be decomposed into cyclonic and anticyclonic components, that is,

$$[\mathbf{DF}] = [C_{\mathrm{dust}} \cdot \mathbf{v}]_{\mathrm{L}} + [C_{\mathrm{dust}} \cdot \mathbf{v}]_{\mathrm{H}} + N, \qquad (2)$$

where the square brackets indicate the time average and the subscripts indicate cyclonic (L) and anticyclonic (H) contributions. The third term $N = [C_{\mathrm{dust}} \cdot \mathbf{v}]_{\mathrm{N}}$ represents the neutral contribution as the residual. The cyclonic and anticyclonic winds are defined herein by the curvature κ_2 defined as follows (Okajima et al. 2021):

$$\kappa_2 \equiv \frac{1}{R_S} = \frac{1}{V^3}\left(-uvu_x + u^2 v_x - v^2 u_y + uvv_y\right), \qquad (3)$$

where R_S is the curvature radius and V is the scalar wind speed. Subscripts x and y denote partial derivatives with respect to the longitude and latitude, respectively. Curvature vorticity (V/R_S) is one of the components of vorticity, together with shear vorticity. Winds accompanied by a positive (negative) curvature with a zero threshold are identified as cyclonic (anticyclonic) winds in the Northern Hemisphere. We can set a non-zero threshold for the curvature (e.g., 0.4×10^{-6} m^{-1} utilized in Okajima et al. 2021) instead of the zero curvature threshold to consider a marginal zone of cyclonic and anticyclonic vortices. If the non-zero curvature threshold is adopted, the third term on the right-hand side of Eq. (2) remains. Whereas it vanishes under the zero curvature threshold because all grid points are classified into the cyclonic or anticyclonic zone. This discrimination was calculated based on the 6-hourly wind data of JRA-55. The dust data from JRAero were horizontally interpolated into the JRA-55 grid.

3. Results

3.1 Dust emission

First, the dust emission variation was investigated as a factor of the dust deposition variability in Japan. Figure 2 shows the regressed anomalies of dust emission around the Mongolian Plateau, a main source region of the carried dust. At first glance, we notice the similarity between the anomalies regressed on the dust deposition variabilities in Domains 1 and 2. The positive anomaly in Gobi Desert, which is one of the maxima of the mean emission (magenta contours) around the boundary of China and Mongolia, means that the emission simultaneously increased when the deposition over Japan increased. The peak of the anomaly was found over the east of the climatological maximum of emission in Gobi Desert. The enhanced emission over the main dust source area simply explained the increased deposition in the downstream. This result was consistent with the dust carried to

East Asia originating from Gobi Desert. Interestingly, dust emission over the northeastern portion of the Taklimakan Desert in Tarim Basin northwest of the Tibetan Plateau exhibited a negative correlation, especially for Domain 2. A seesaw-like variability between the Gobi and Taklimakan deserts in the interannual timescale was implied.

The dust storms over the Mongolian Plateau are controlled not only by the surface wind speed but also by the land surface conditions (Kurosaki and Mikami 2003, 2004, 2005; Zou and Zhai 2004; Ding et al. 2005; Lee and Sohn 2011; Song et al. 2016). Kurosaki and Mikami (2005) showed that the strong surface wind is a major factor in the desert regions, whereas the vegetation determines dust outbreaks over the grassland regions. They also assessed the snow cover contributions. Consequently, the combined effects of anomalous winds and the land surface conditions, such as vegetation, snow cover, and soil moisture, are responsible for the dust emission variation over the Mongolian Plateau. Section 3.2 discusses the modulated wind fields.

3.2 Anomalous atmospheric circulation

Our main interest is to investigate the relationship between dust deposition variability and atmospheric circulation. Figures 3a and b show the regressed anomalies of the sea level pressure (SLP) and surface winds associated with the dust deposition variation in Japan based on the monthly mean data. The cyclonic circulation anomaly appears over Japan when the dust deposition increases, accompanied by the anticyclonic anomaly over the Kamchatka Peninsula. These features were roughly the same between Domains 1 and 2. However, as for Domain 1, the significant westerly anomalies south of Japan corresponding to the southern margin of the anomalous cyclone were widely dominant over southwestern Japan. The significance of surface westerly anomaly is confirmed also in the Domain 2 variation (Fig. 3b).

Figures 3c–f depict the anomalies of the geopotential height, winds, and dust concentration at 700 hPa. Overall, the anomalies associated with the dust deposition variations in the Domains 1 and 2 are similar. The high dust concentrations over the region from the northwest of the Tibetan Plateau via Japan to the western North Pacific were consistent with the enhanced dust emission (Fig. 2) and subsequently increased the dust deposition. An anomalous trough over the northwest of the Japanese islands tilting westward with altitude exhibited a baroclinic structure. The related intensification of the cyclonic winds (Figs. 3e and f) was responsible for the higher-than-normal dust concentrations through dust transport from its source region. Indeed, comparing each analysis year (Fig. S1), the higher concentration of dust distributes over the southern rim of the cyclonic anomalies such as the 2012 and 2013 cases. In contrast, the anomalous ridge over East Asia accompanied lower concentrations of dust such as in the 2014 case. These results indicate the significant impacts of the anomalous westerlies on the dust transport from the Mongolian Plateau to Japan.

If we pay attention to the difference between the circulation anomalies associated with the Domains 1 and 2 variations, the anomalous trough in the Domain 1 anomaly was centered at the eastern coast of the Asian continent (Fig. 3c), and significant wind anomalies (purple vectors) were only toward western Japan (Fig. 3e). Meanwhile, the cyclonic anomaly of Domain 2 shifted northwestward from that of Domain 1 (Fig. 3d), and significant wind anomalies were toward northern Japan (Fig. 3f). Figure 4 shows the difference between the regressed anomalies associated with Domains 1 and 2 variabilities. Note that the figure plotted is the anomaly of the Domain 2 variation minus that of the Domain 1 variation, highlighting the Domain 2 anomaly. The SLP anomaly associated with the variation in Domain 2 is lower over the East Asian continent (Fig. 4a). As for the difference at 700 hPa (Fig. 4b), the noteworthy negative anomaly over the eastern Siberia continent indicates the anomalous trough in the Domain 2 variability is deeper than that of Domain 1. This slightly different position and intensity of the anomalous trough may explain the dust deposition variability between Domains 1 and 2.

Figures 5a and b show the altitude–longitude cross-sections of the dust concentration and the winds averaged over 30–35°N and 35–45°N, which are across Domains 1 and 2, respectively, to assess the vertical structure of the abovementioned anomalies. The dust concentrations were higher than normal, especially over the eastern foot of the Tibetan Plateau. Moreover, the anomalous westerlies were indicative of the intensified eastward dust transport (Fig. 5a). The anomalous descent was significantly confirmed over 120–140°E in the lower to middle troposphere, which may be favorable to dust deposition. As for the crosssection along with the dust source regions toward Domain 2 (Fig. 5b), the higher-than-normal dust concentration over the western Mongolian Plateau (Gobi Desert; 100–120°E) was consistent with the anomalous dust emission (Fig. 2). In contrast, the dust concentration decreased over Taklimakan Desert (85–95°E). The eastward anomalies of the mid-tropospheric winds transported more dust from the source area to Japan. Here, one may notice the statistically non-significant anomaly of dust concentration in the lower troposphere just over Japan (~130–140°E). This may be related to both enhanced removal and transport processes. When the dust is removed from the atmosphere and deposited on the ground surface, the dust concentration decreases in the atmosphere just over the region if the dust was not carried from other regions. While our results showed that the dust was anomalously transported from the Mongolian Plateau, contributing to the increase in dust concentration. The complex processes for aerosol may be responsible for the non-significant anomalies of the dust concentration in the lower troposphere over Japan.

3.3 Transient cyclone activity

Although the stationary component variability was mainly discussed in the preceding sections based on the monthly mean data, the transient eddy activity is investigated in this subsection. Extratropical cyclones are an important factor in the springtime dust storms over East Asia (Qian et al. 2002b; Minamoto et al. 2018). In the present study, we utilized the local deepening rate (LDR: Kuwano-Yoshida 2014) representing the differentiation of the surface pressure per unit time to diagnose its monthly mean activity. The LDR estimated by the 24 h central difference (LDR24) is defined as follows:

$$\mathrm{LDR24} = -\frac{p(t+12h) - p(t-12h)}{24}\left|\frac{\sin 60°}{\sin\theta}\right|, \qquad (4)$$

where p is the surface pressure, t is the time, and θ is the grid point latitude. We used the 6-hourly surface pressure of JRA-55 for the calculation. The threshold for the time averages of the positive LDR24 was set at 0.5 hPa h^{-1} to extract comparatively rapid deepening lows. LDR24P0.5 denotes the time average of LDR24 ≥ 0.5 hPa h^{-1} with all other values set to 0. Note that it is more lenient than the typical threshold for explosively developing (bomb) cyclones (LDR24P1).

Figure 6 shows the mean LDR24P0.5 and its anomaly associated with the dust deposition variation over Japan, which were applied with weak horizontal smoothing. In the climatological mean state (black contours), extratropical cyclones tended to develop over the east of Japan, roughly corresponding to the "storm track" in spring (Chen et al. 1991; Hayasaki and Kawamura 2012). In the variability for Domain 2 (Fig. 6b), the significant positive anomalies of the transient cyclone activity were evident around Japan, indicating the enhancement of the cyclone activity when a larger-than-normal amount of dust is deposited in northern Japan. The distribution of the positive LDR anomaly well regionally corresponds to the maximum developing points of bomb cyclones associated with the Kuroshio Current (Yoshiike and Kawamura 2009; Hirata et al. 2016) as well as springtime extratropical cyclones (Hayasaki and Kawamura 2012). This result may imply that explosively developing cyclones, that are subsequently located over the northeast of Japan, can carry the dust more northward in comparison with the non-significant anomalies for the Domain 1 variability (Fig. 6a). In contrast, the extratropical cyclone activity was suppressed over the center of its climatological maximum (negative regression coefficients in Fig. 6). The northeast–southwest pair of the negative and positive LDR anomalies was consistent with the SLP anomalies (Figs. 3a and b). It is suggested that the anomalous extratropical cyclone activity may be also responsible for the increase of the dust concentration and deposition around Japan through the intensified dust transport.

3.4 Dust behavior under cyclonic and anticyclonic vortices

The preceding sections suggested that the dust transport by the middle- to lower-tropospheric winds plays an essential role in the dust deposition and concentration variability over East Asia. Although the cyclonic flows and activity were mainly examined considering the accompanied strong winds when focusing on the emission and transport processes (e.g., Fig. 6; Qian et al. 2002b; Kawai et al. 2015, 2018; Minamoto et al. 2018), the discussion on anticyclones has been conventionally neglected. The cyclonic and anticyclonic contributions to the dust transport will be discussed separately herein based on the discrimination using the curvature of winds [Eq. (3)].

Figures 7a and b show the mean cyclonic and anticyclonic dust fluxes at 700 hPa with the zero curvature threshold, respectively. Note that the time averages included zero values.

The total dust flux (i.e., cyclonic plus anticyclonic fluxes; Fig. S2a) indicates the eastward dust transport, as shown by Zhao et al. (2006). Both the cyclonic and anticyclonic fluxes were eastward in the midlatitude, and their magnitude exhibited eastward negative gradients over East Asia. The cyclonic contribution was slightly larger than the anticyclonic one around the region from the Korean Peninsula to the Sea of Japan (estimated as approximately 50–65 % relative to the total flux magnitude), suggesting that the anticyclonic winds are not neglectable in the mean dust transport in coastal East Asia. These features were almost consistent with the results in the case of the non-zero curvature threshold (0.4×10^{-6} m^{-1}) shown in Fig. S2. The non-curvature dust flux in the marginal zone was also eastward (Fig. S2b). This neutral contribution was smaller than the cyclonic contribution (Fig. S2c) but larger than the anticyclonic (Fig. S2d) around East Asia.

Figures 7c–f depict the anomalous dust fluxes regressed onto the interannual variability of dust deposition in Japan. The cyclonic dust flux from Gobi Desert via the Korean Peninsula to Japan was significantly intensified (Figs. 7c and e), bearing resemblance to the stationary wind anomalies (Fig. 3). The slight regional difference of the significant zonal flux anomalies between Domains 1 and 2 (gray shading, Figs. 7c and e) could be responsible for each regional increase of dust deposition. The anticyclonic dust flux also seemed to be stronger than normal, especially in the Domain 2 variation (Fig. 7f). However, we cannot find significant anomalies for the Domain 1 variation (Fig. 7d). Figure 7f implies that anticyclonic vortices were also important players in the dust transport and resultant deposition to northern Japan, together with the cyclonic ones. The results with the non-zero curvature threshold indicated the almost same features (Figs.S2e–h).

We also assessed the dust emission and deposition under cyclonic and anticyclonic vortices. Figure 8a shows the proportion of dust emission under cyclonic surface vortices to the climatological mean. The curvature threshold was set at 0 here; hence, the local residuals represented the corresponding probability under anticyclonic vortices. The surface curvature was obtained from the winds 10 m above the ground of JRA-55. The warm color shading around the eastern Gobi Desert shows that almost all amounts of dust were emitted in association with cyclonic winds. This result is consistent with the cyclonic winds being generally stronger and the subsequent dust storm frequency (Kurosaki and Mikami 2003, 2005). Moreover, previous studies investigating extreme dust events demonstrated an essential role of extratropical cyclones and related cold fronts in dust emission over Gobi Desert (Kawai et al. 2015; Kai et al. 2021) as well as the transport to Japan (Minamoto et al. 2018). Meanwhile, over northeastern Taklimakan Desert in Tarim Basin, the anticyclonic contribution almost accounted for the mean dust emission. Taklimakan Desert is surrounded by mountains, except on its northeastward side (thick black contours). Aoki et al. (2005) showed an intruding course of surface winds into the Tarim Basin accompanied by an anticyclonic curvature and coldness associated with the topographic effect. Thus, this topography may cause the anticyclonic distributions.

Figures 8b and c show the climatological mean and the proportion of wet and dry dust depositions, respectively, under cyclonic curvature at 850 hPa, which generally captures the synoptic-scale eddies. The climatological mean of wet deposition (white contours, Fig. 8b) bore a striking resemblance to the whole mean deposition (Fig. 1a), implying that the wet process is dominant for the dust deposition around Japan. The local residuals of the proportion (shading) corresponded to the anticyclonic vortices. Both the wet and dry dust depositions mainly occur under the cyclonic vortices, especially over the sea and northeastern China, where the main track of synoptic-scale cyclones can be observed in spring (Chen et al. 1991). The larger contribution of the cyclonic vortices is consistent with the intensified extratropical cyclone activity when dust deposition and/or dust storms increase (Fig. 6; Qian et al. 2002b). However, the cyclonic and anticyclonic contributions are locally fifty-fifty (green shading), indicating that the anticyclones could be treated as a responsible factor for dust deposition in Japan.

To discuss the suggestion, we show a case with an anticyclone playing an essential role in dust transport and deposition (Fig. S3). In this example, a large amount of dust was clockwise carried around the northern margin of an eastward-moving anticyclone near the Korean Peninsula. The carried dust was subsequently deposited in northern Japan through the wet process. The accompanying rainfall may be associated with the preceding developing cyclone. This case indicates that the baroclinic instability waves are important in the whole dust behavior process, especially in transportation and deposition, and supports the aforementioned results.

4. Summary and discussion

This study investigated the anomalous atmospheric circulation fields associated with the interannual variability of dust deposition in Japan during the spring season using the global aerosol reanalysis dataset. In the larger-than-normal deposited dust years, an anomalous trough emerged over the East Asian continent toward the northwest of Japan in the mid-troposphere, transporting dust from the Mongolian Plateau via the Korean Peninsula to Japan. The enhanced emission around Gobi Desert supported this process. The intensified extratropical cyclone activity was consistent with the negative SLP anomaly around Japan, implying more frequent dust storms. The locally different dust variation between Domains 1 (western Japan) and 2 (northern Japan) seemed to be caused by the slightly shifted anomalous flows. Differences in sensitivity to the transient eddy activity and anticyclonic dust transport were also recognized. We further examined the dust behavior under cyclonic and anticyclonic vortices and found that the cyclonic contribution for the mean dust transport was slightly larger compared with the anticyclonic contribution, but the anticyclonic transport of dust was not neglected especially for the Domain 2 variability. The dust emission around Gobi Desert mainly occurred under the surface cyclonic vortices, whereas that over Taklimakan Desert was an outbreak under the anticyclonic vortices caused by their unique topography. The dust deposition was mainly under cyclonic vortices; however, the dust deposition under anticyclonic vortices could not be neglected.

Although we attempted to clarify the interannual variability of dust in East Asia using the full period of the JRAero dataset, the analysis period in the present study may be short. Moreover, it has been pointed out that the global climate models include a bias about the wet removal process associated with the reproducibility of rainfall (Wang et al. 2021). To treat these problems, we further investigated the interannual variability using the long-term dust observations by JMA from 1967 to 2022. Figure 9a depicts the interannual time series of the number of days that dust was observed at any point of the 11 observation stations in Japan. The top 20% of the most frequent years were selected and their composited circulation anomaly at 700 hPa is shown in Figure 9b. The significant cyclonic anomaly over the Siberian continent towards northeastern China bears striking resemblance to the modulated atmospheric circulation fields in JRAero (Figs. 3c–f). The intensified westerlies from the Mongolian Plateau to Japan were responsible for the enhanced dust transport and the resultant high frequency of dust observation. This process may involve the mechanisms mentioned in Section 3, supporting our results using JRAero. We further analyzed the difference between western and northern Japan variability using the JMA observation (Fig. S4). The results classifying the 11 observation stations into western and northern Japan supported the significance of the deepened trough over the Siberian continent towards northeastern China and the related strong dust transport by westerlies (Fig. S4b, c).

It is well known that interannual climate variability is highly affected by global teleconnections, such as the Arctic Oscillation (AO) and El Niño–Southern Oscillation

(ENSO). Gong et al. (2006a) pointed out a possible impact of AO on the variation of dust storm frequency in northern China. We calculated correlation coefficients using the long-term dust observations by JMA in April from 1967 to 2022. Here, the AO index in April and the springtime (MAM-mean) Niño3.4 index representing the ENSO phase were obtained from NOAA Climate Prediction Center [https://origin.cpc.ncep.noaa.gov/]. The simultaneous correlation coefficient between the AO index and the number of dust observed days in Japan was −0.107, indicating a weak correlation. The same could be said for the results when the observation stations are classified into western and northern Japan ($r = -0.082$ and $r = -0.048$, respectively). Whereas the correlation coefficient with the Niño3.4 index was 0.153, 0.140, and 0.172 in whole, western, and northern Japan, respectively. These results suggest that it may be difficult to say a robust linkage between the dust observation in Japan and AO as well as ENSO only from our results obtained through the analyses for the simultaneous relationship. However, we should not neglect the great influences of the teleconnection patterns on the circulation and precipitation variabilities over East Asia. These influences can be memorized in the land surface condition and affect the dust variability with monthly- to seasonal-scale time lag. It is still a controversial problem and necessary to examine carefully in further study.

As for the analysis of the extratropical cyclones, our result implied a relationship between bomb cyclones and the dust deposition variation in Japan (Fig. 6). To verify the influence of bomb cyclones on dust transport to northern Japan is awaited. Furthermore, recent studies focusing on dust events in Europe or Middle East showed a relationship between dust transport and an atmospheric river (referred to as a dusty atmospheric river) (Dezfuli et al. 2021; Francis et al. 2022). Because East Asia is also one of the regions where atmospheric rivers are frequently observed (Kamae et al. 2017), their association is an interesting problem.

The environmental impacts of aerosols on deposition (nutrients, neutralization, and snow-albedo feedback), surface air concentration (toxicity and visibility), and upper troposphere (regional climate) differ from each other. The environmental impacts also differ depending on species (dust, sulfate, carbonaceous, sea-salt, etc.). The current analysis to relate atmospheric circulation fields and its constituent behaviors for different quantities (deposition/concentration of different species) will be interesting. The reanalysis period of JRAero is now planned to extend (currently extended to 2019) but the version we used in this study provided seven years (2011–2017). On the other hand, other aerosol reanalyses such as the Copernicus Atmosphere Monitoring Service (CAMS) reanalysis (2003–2021; Inness et al. 2019) and the Modern-Era Retrospective analysis for Research and Applications Version 2 (MERRA-2) (1980–; Gelaro et al. 2017) provide longer periods of reanalysis data. To enhance the robustness of current findings, a similar study using other aerosol reanalysis data for longer periods will be needed. This study only focused on mid-spring; hence, the other seasons will be examined in upcoming work.

Data Availability Statement

The JRA-55 datasets are provided by JMA and available at https://jra.kishou.go.jp/JRA-55/index_en.html (last accessed: August 23, 2022). The JRAero datasets are by MRI and the Research Institute for Applied Mechanics (RIAM) of Kyushu University and are available at https://www.riam.kyushu-u.ac.jp/taikai/JRAero/index.html (last accessed: August 23, 2022). The dust observations by JMA are available at https://www.data.jma.go.jp/gmd/env/kosahp/kosa_data_index.html (in Japanese; last accessed: August 23, 2022).

Supplement

Supplement 1 shows the anomalies of geopotential height and dust concentration at 700 hPa in each year from 2011 to 2017. Supplement 2 shows the mean total dust flux at 700 hPa, the non-zero curvature threshold fluxes, and their regressed anomalies. Supplement 3 shows a case of dust events associated with an anticyclone on April 15, 2016. Supplement 4 shows the composited circulation anomaly at 700 hPa using the JMA observation classified into western and northern Japan.

Acknowledgments

The authors are grateful to the two anonymous reviewers for their constructive comments on the earlier version of this paper. This research was supported by the Fundamental

Technology Research of MRI (M5), the Japanese Society for the Promotion of Sciences (JSPS) KAKENHI (grant nos. JP19H01155 and JP22H00562), the Environmental Research and Technology Development Fund from the Environmental Restoration and Conservation Agency (ERCA) (grant nos. JPMEERF20215003 and JPMEERF20205001), and Arctic Challenge for Sustainability II (ArCS II) (grant no. JPMXD1420318865) from the Ministry of Education, Culture, Sports, Sciences, and Technology (MEXT).

References

Aoki, I., Y. Kurosaki, R. Osada, T. Sato, and F. Kimura, 2005: Dust storms generated by mesoscale cold fronts in the Tarim Basin, Northwest China. *Geophys. Res. Lett.*, **32**, L06807, doi:10.1029/2004GL021776.

Chen, S. J., Y. H. Kuo, P. Z. Zhang, and Q. F. Bai, 1991: Synoptic climatology of cyclogenesis over East Asia, 1958-1987. *Mon. Wea. Rev.*, **119**, 1407–1418.

Dezfuli, A., M. G. Bosilovich, and D. Barahona, 2021: A dusty atmospheric river brings floods to the Middle East. *Geophys. Res. Lett.*, **48**, e2021GL095441, doi:10.1029/2021GL095441.

Di Mauro, B., R. Garzonio, M. Rossini, G. Filippa, P. Pogliotti, M. Galvagno, U. Morra di Cella, M. Migliavacca, G. Baccolo, M. Clemenza, B. Delmonte, V. Maggi, M. Dumont, F. Tuzet, M. Lafaysse, S. Morin, E. Cremonese, and R. Colombo, 2019: Saharan dust events in the European Alps: role in snowmelt and geochemical characterization. *The Cryosphere*, **13**, 1147–1165.

Ding, R., J. Li, S. Wang, and F. Ren, 2005: Decadal change of the spring dust storm in northwest China and the associated atmospheric circulation. *Geophys. Res. Lett.*, **32**, L02808, doi:10.1029/2004GL021561.

Francis, D., R. Fonseca, N. Nelli, D. Bozkurt, G. Picard, and B. Guan, 2022: Atmospheric rivers drive exceptional Saharan dust transport towards Europe. *Atmos. Res.*, **266**, 105959, doi:10.1016/j.atmosres.2021.105959.

Gelaro, R., and co-authors, 2017: The modern-era retrospective analysis for research and applications, version 2 (MERRA-2). *J. Climate*, **30**, 5419–5454.

Gong, D. Y., R. Mao, and Y. D. Fan, 2006a: East Asian dust storm and weather disturbance: possible links to the Arctic Oscillation. *Int. J. Climatol.*, **26**, 1379–1396.

Gong, S. L., X. Y. Zhang, T. L. Zhao, X. B. Zhang, L. A. Barrie, I. G. McKendry, and C. S. Zhao, 2006b: A simulated climatology of Asian dust aerosol and its trans-Pacific transport. Part II: Interannual variability and climate connections. *J. Climate*, **19**, 104–122.

Han, Y., X. Fang, S. Kang, H. Wang, and F. Kang, 2008: Shifts of dust source regions over central Asia and the Tibetan Plateau: Connections with the Arctic oscillation and the westerly jet. *Atmos. Environ.*, **42**, 2358–2368.

Hashizume, M., Y. Kim, C. F. S. Ng, Y. Chung, L. Madaniyazi, M. L. Bell, Y. L. Guo, H. Kan, Y. Honda, S.-M. Yi, H. Kim, and Y. Nishiwaki, 2020: Health effects of Asian dust: A systematic review and meta-analysis. *Environ. Health Perspect.*, **128**, 066001, doi:10.1289/EHP5312.

Hayasaki, M., and R. Kawamura, 2012: Cyclone activities in heavy rainfall episodes in Japan during spring season. *SOLA*, **8**, 45–48.

Hirata, H., R. Kawamura, M. Kato, and T. Shinoda, 2016: Response of rapidly developing extratropical cyclones to sea surface temperature variations over the western Kuroshio–Oyashio confluence region. *J. Geophys. Res.: Atmos.*, **121**, 3843–3858.

Hu, Z., J. Huang, C. Zhao, J. Bi, Q. Jin, Y. Qian, L.R. Leung, T. Feng, S. Chen, and J. Ma, 2019: Modeling the contributions of Northern Hemisphere dust sources to dust outflow from East Asia. *Atmos. Environ.*, **202**, 234–243.

Inness, A., and co-authors, 2019: The CAMS reanalysis of atmospheric composition. *Atmos. Chem. Phys.*, **19**, 3515–3556.

Inomata, Y., Y. Igarashi, M. Mikami, T. Y. Tanaka, and M. Chiba, 2009: Seasonal and yearly variations of dust deposition in Tsukuba: Possible linkage with variations of dust emission over the Asian continent. *SOLA*, **5**, 153–156.

Iwasaka, Y., H. Minoura, and K. Nagaya, 1983: The transport and spacial scale of Asian dust-storm clouds: a case study of the dust-storm event of April 1979. *Tellus B*, **35**, 189–196.

Kai, K., K. Kawai, A. Ito, Y. Aizawa, Y. Minamoto, E. Munkhjargal, and E. Davaanyam, 2021: Dust hotspot in the Gobi Desert: A field survey in April 2019. *SOLA*, **17**, 130–133.

Kamae, Y., W. Mei, S.-P. Xie, M. Naoi, and H. Ueda, 2017: Atmospheric rivers over the

Northwestern Pacific: Climatology and interannual variability. *J. Climate*, **30**, 5605–5619.

Kameda, T., E. Azumi, A. Fukushima, N. Tang, A. Matsuki, Y. Kamiya, A. Toriba, and K. Hayakawa, 2016: Mineral dust aerosols promote the formation of toxic nitropolycyclic aromatic compounds. *Sci. Rep.*, **6**, 24427, doi:10.1038/srep24427.

Kang, L., J. Huang, S. Chen, and X. Wang, 2016: Long-term trends of dust events over Tibetan Plateau during 1961–2010. *Atmos. Environ.*, **125**, 188–198.

Kawai, K., K. Kai, Y. Jin, N. Sugimoto, and D. Batdorj, 2015: Dust event in the Gobi Desert on 22-23 May 2013: Transport of dust from the atmospheric boundary layer to the free troposphere by a cold front. *SOLA*, **11**, 156–159.

Kawai, K., K. Kai, Y. Jin, N. Sugimoto, and D. Batdorj, 2018: Lidar network observation of dust layer development over the Gobi Desert in association with a cold frontal system on 22–23 May 2013. *J. Meteor. Soc. Japan*, **96**, 255–268.

Kim, J., 2008: Transport routes and source regions of Asian dust observed in Korea during the past 40 years (1965–2004). *Atmos. Environ.*, **42**, 4778–4789.

Kobayashi, S., Y. Ota, Y. Harada, A. Ebita, M. Moriya, H. Onoda, K. Onogi, H. Kamahori, C. Kobayashi, H. Endo, K. Miyaoka, and K. Takahashi, 2015: The JRA-55 reanalysis: general specifications and basic characteristics. *J. Meteor. Soc. Japan*, **93**, 5–48.

Kurosaki, Y., and M. Mikami, 2003: Recent frequent dust events and their relation to surface wind in East Asia. *Geophys. Res. Lett.*, **30**, 1736, doi:10.1029/2003GL017261.

Kurosaki, Y., and M. Mikami, 2004: Effect of snow cover on threshold wind velocity of dust outbreak. *Geophys. Res. Lett.*, **31**, L03106, doi:10.1029/2003GL018632.

Kurosaki, Y., and M. Mikami, 2005: Regional difference in the characteristic of dust event in East Asia: Relationship among dust outbreak, surface wind, and land surface condition. *J. Meteor. Soc. Japan*, **83**, 1–18.

Kuwano-Yoshida, A., 2014: Using the local deepening rate to indicate extratropical cyclone activity. *SOLA*, **10**, 199–203.

Lee, E. H., and B. J. Sohn, 2011: Recent increasing trend in dust frequency over Mongolia and Inner Mongolia regions and its association with climate and surface condition change. *Atmos. Environ.*, **45**, 4611–4616.

Lee, H. N., Y. Igarashi, M. Chiba, M. Aoyama, K. Hirose, and T. Tanaka, 2006: Global model simulations of the transport of Asian and Sahara dust: Total deposition of dust mass in Japan. *Water Air Soil Pollut.*, **169**, 137–166.

Littmann, T., 1991: Dust storm frequency in Asia: Climatic control and variability. *Int. J. Climatol.*, **11**, 393–412.

Liu, X., Z. Y. Yin, X. Zhang, and X. Yang, 2004: Analyses of the spring dust storm frequency of northern China in relation to antecedent and concurrent wind, precipitation, vegetation, and soil moisture conditions. *J. Geophys. Res.: Atmos.*, **109**, D16210, doi:10.1029/2004JD004615.

Matsuki, A., Y. Iwasaka, K. Osada, K. Matsunaga, M. Kido, Y. Inomata, D. Trochkine, C. Nishita, T. Nezuka, T. Sakai, D. Zhang, and S. A. Kwon, 2003: Seasonal dependence of the long-range transport and vertical distribution of free tropospheric aerosols over east Asia: On the basis of aircraft and lidar measurements and isentropic trajectory analysis. *J. Geophys. Res.: Atmos.*, **108**, 8663, doi:10.1029/2002JD003266.

Minamoto, Y., K. Nakamura, M. Wang, K. Kawai, K. Ohara, J. Noda, E. Davaanyam, N. Sugimoto, and K. Kai, 2018: Large-scale dust event in East Asia in May 2017: Dust emission and transport from multiple source regions. *SOLA*, **14**, 33–38.

Ninomiya, K., 1968: Heat and water budget over the Japan Sea and the Japan Islands in winter season with special emphasis on the relation among the supply from sea surface, the convective transfer and the heavy snowfall. *J. Meteor. Soc. Japan*, **46**, 343–372.

Niwano, M., M. Kajino, T. Kajikawa, T. Aoki, Y. Kodama, T. Tanikawa, and S. Matoba, 2021: Quantifying relative contributions of light-absorbing particles from domestic and foreign sources on snow melt at Sapporo, Japan during the 2011–2012 winter. *Geophys. Res. Lett.*, **48**, e2021GL093940, doi:10.1029/2021GL093940.

Okajima, S., H. Nakamura, and Y. Kaspi, 2021: Cyclonic and anticyclonic contributions to atmospheric energetics. *Sci. Rep.*, **11**, 1–10.

Onishi, K., Y. Kurosaki, S. Otani, A. Yoshida, N. Sugimoto, and Y. Kurozawa, 2012: Atmospheric transport route determines components of Asian dust and health effects in Japan. *Atmos. Environ.*, **49**, 94–102.

Parungo, F., Z. Li, X. Li, D. Yang, and J. Harris, 1994: Gobi dust storms and the Great Green Wall. *Geophys. Res. Lett.*, **21**, 999–1002.

Perez, L., A. Tobias, X. Querol, N. Künzli, J. Pey, A. Alastuey, M. Viana, N. Valero, M. González-Cabré, and J. Sunyer, 2008: Coarse particles from Saharan dust and daily mortality, *Epidemiology*, **19**, 800–807.

Qian, W., H.-S. Kang, and D.-K. Lee, 2002a: Distribution of seasonal rainfall in the East Asian monsoon region. *Theor. Appl. Climatol.*, **73**, 151–168.

Qian, W., L. Quan, and S. Shi, 2002b: Variations of the dust storm in China and its climatic control. *J. Climate*, **15**, 1216–1229.

Rastogi, N., and M. M. Sarin, 2006: Chemistry of aerosols over a semi-arid region: Evidence for acid neutralization by mineral dust. *Geophys. Res. Lett.*, **33**, L23815.

Ridgwell, A. J., 2002: Dust in the Earth system: the biogeochemical linking of land, air and sea. *Philos. Trans. Royal. Soc. A*, **360**, 2905–2924.

Shimizu, A., N. Sugimoto, I. Matsui, K. Arao, I. Uno, T. Murayama, N. Kagawa, K. Aoki, A. Uchiyama, and A. Yamazaki, 2004: Continuous observations of Asian dust and other aerosols by polarization lidars in China and Japan during ACE-Asia. *J. Geophys. Res.: Atmos.*, **109**, D19S17, doi:10.1029/2002JD003253.

Song, H., K. Zhang, S. Piao, and S. Wan, 2016: Spatial and temporal variations of spring dust emissions in northern China over the last 30 years. *Atmos. Environ.*, **126**, 117–127.

Stafoggia, M., S. Zauli-Sajani, J. Pey, E. Samoli, E. Alessandrini, X. Basagaña, A. Cernigliaro, M. Chiusolo, M. Demaria, J. Díaz, A. Faustini, K. Katsouyanni, A.G. Kelessis, C. Linares, S. Marchesi, S. Medina, P. Pandolfi, N. Pérez, X. Querol, G. Randi, A. Ranzi,

A. Tobias, F. Forastiere, and MED-PARTICLES Study Group. 2016: Desert dust outbreaks in Southern Europe: contribution to daily PM10 concentrations and short-term associations with mortality and hospital admissions. *Environ. Health Perspect.*, **124**, 413–419.

Steenburgh, W. J., and S. Nakai, 2020: Perspectives on sea-and lake-effect precipitation from Japan's "Gosetsu Chitai". *Bull. Amer. Meteor. Soc.*, **101**, E58–E72.

Sun, J., M. Zhang, and T. Liu, 2001: Spatial and temporal characteristics of dust storms in China and its surrounding regions, 1960–1999: Relations to source area and climate. *J. Geophys. Res.: Atmos.*, **106**, 10325–10333.

Szopa, S., V. Naik, B. Adhikary, P. Artaxo, T. Berntsen, W.D. Collins, S. Fuzzi, L. Gallardo, A. Kiendler-Scharr, Z. Klimont, H. Liao, N. Unger, and P. Zanis, 2021: Short-Lived Climate Forcers. In *Climate Change 2021: The Physical Science Basis. Contribution of Working Group I to the Sixth Assessment Report of the Intergovernmental Panel on Climate Change* [Masson-Delmotte, V., P. Zhai, A. Pirani, S.L. Connors, C. Pean, S. Berger, N. Caud, Y. Chen, L. Goldfarb, M.I. Gomis, M. Huang, K. Leitzell, E. Lonnoy, J.B.R. Matthews, T.K. Maycock, T. Waterfield, O. Yelekci, R. Yu, and B. Zhou (eds.)]. Cambridge University Press, Cambridge, United Kingdom and New York, NY, USA, pp. 817-922, doi:10.1017/9781009157896.008.

Tanaka, T. Y., K. Orito, T. T. Sekiyama, K. Shibata, M. Chiba, and H. Tanaka, 2003: MASINGAR, a global tropospheric aerosol chemical transport model coupled with

MRI/JMA98GCM: Model description. *Pap. Meteor. Geophys.*, **53**, 119–138.

Tanaka, T. Y., and M. Chiba, 2005: Global simulation of dust aerosol with a chemical transport model, MASINGAR. *J. Meteor. Soc. Japan*, **83A**, 255–278.

Tanaka, T. Y., and M. Chiba, 2006: A numerical study of the contributions of dust source regions to the global dust budget. *Global Planet. Change*, **52**, 88–104.

Terada, H., H. Ueda, and Z. Wang, 2002: Trend of acid rain and neutralization by yellow sand in east Asia—a numerical study. *Atmos. Environ.*, **36**, 503–509.

Tsunematsu, N., T. Sato, F. Kimura, K. Kai, Y. Kurosaki, T. Nagai, H. Zhou, and M. Mikami, 2005: Extensive dust outbreaks following the morning inversion breakup in the Taklimakan Desert. *J. Geophys. Res.: Atmos.*, **110**, D21207, doi:10.1029/2005JD005994.

Ueda, H., 2005: Air-sea coupled process involved in stepwise seasonal evolution of the Asian summer monsoon. *Geograph. Rev. of Japan*, **78**, 825–841.

Ueda, H., M. Ohba, and S.-P. Xie, 2009: Important factors for the development of the Asian-Northwest Pacific summer monsoon. *J. Climate*, **22**, 649–669.

Uno, I., K. Eguchi, K. Yumimoto, T. Takemura, A. Shimizu, M. Uematsu, Z. Liu, Z. Wang, Y. Hara, and N. Sugimoto, 2009: Asian dust transported one full circuit around the globe. *Nat. Geosci.*, **2**, 557–560.

Wang, X., J. Huang, M. Ji, and K. Higuchi, 2008: Variability of East Asia dust events and their long-term trend. *Atmos. Environ.*, **42**, 3156–3165.

Wang, Y., W. Xia, X. Liu, S. Xie, W. Lin, Q. Tang, H.-Y. Ma, Y. Jiang, B. Wang, and G. J.

Zhang, 2021: Disproportionate control on aerosol burden by light rain. *Nat. Geosci.*, **14**, 72–76.

Yang, Y. Q., Q. Hou, C. H. Zhou, H. L. Liu, Y. Q. Wang, and T. Niu, 2008: Sand/dust storm processes in Northeast Asia and associated large-scale circulations. *Atmos. Chem. Phys.*, **8**, 25–33.

Yoshiike, S., and R. Kawamura, 2009: Influence of wintertime large-scale circulation on the explosively developing cyclones over the western North Pacific and their downstream effects. *J. Geophys. Res.: Atmos.*, **114**, D13110, doi:10.1029/2009JD011820.

Yukimoto, S., Y. Adachi, M. Hosaka, T. Sakami, H. Yoshimura, M. Hirabara, T. Y. Tanaka, E. Shindo, H. Tsujino, M. Deushi, R. Mizuta, S. Yabu, A. Obata, H. Nakano, T. Koshiro, T. Ose, and A. Kitoh, 2012: A new global climate model of the Meteorological Research Institute: MRI-CGCM3 –Model description and basic performance. *J. Meteorol. Soc. Japan*, **90A**, 23–64.

Yumimoto, K., T. Y. Tanaka, N. Oshima, and T. Maki, 2017: JRAero: the Japanese reanalysis for aerosol v1.0. *Geosci. Model Dev.*, **10**, 3225–3253.

Yumimoto, K., M. Kajino, T. Y. Tanaka, and I. Uno, 2019: Dust vortex in the Taklimakan Desert by Himawari-8 high frequency and resolution observation. *Sci. Rep.*, **9**, 1209, doi:10.1038/s41598-018-37861-4.

Zhang, D., Y. Iwasaka, G. Shi, J. Zang, A. Matsuki, and D. Trochkine, 2003: Mixture state and size of Asian dust particles collected at southwestern Japan in spring 2000. *J.*

Geophys. Res.: Atmos., **108**, 4760, doi:10.1029/2003JD003869.

Zhang, C., H. Gao, X. Yao, Z. Shi, J. Shi, Y. Yu, L. Meng, and X. Guo, 2018: Phytoplankton growth response to Asian dust addition in the northwest Pacific Ocean versus the Yellow Sea. *Biogeosciences*, **15**, 749–765.

Zhao, T. L., S. L. Gong, X. Y. Zhang, J. P. Blanchet, I. G. McKendry, and Z. J. Zhou, 2006: A simulated climatology of Asian dust aerosol and its trans-Pacific transport. Part I: Mean climate and validation. *J. Climate*, **19**, 88–103.

Zou, X. K., and P. M. Zhai, 2004: Relationship between vegetation coverage and spring dust storms over northern China. *J. Geophys. Res.: Atmos.*, **109,** D03104, doi:10.1029/2003JD003913.

List of Figures

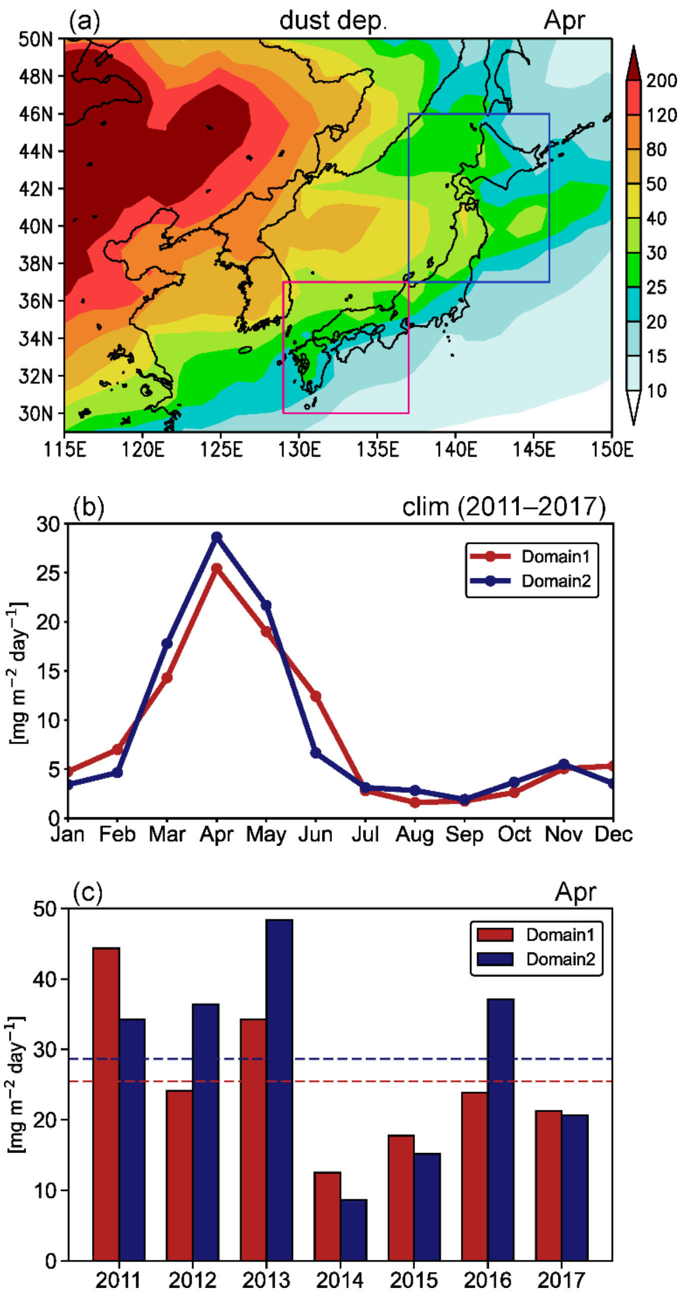

Fig. 1 (a) Mean total dust deposition in April from 2011 to 2017. (b) Seasonal time series of 2011–2017-mean dust deposition averaged over the land in Domains 1 [30–37°N, 129–137°E] and 2 [37–46°N, 137–146°E]. (c) Similar to (b), but for interannual time series in April from 2011 to 2017. In (c), dashed lines denote the average in each domain. Units: mg m^{-2} day^{-1}. The rectangles in panel (a) indicate Domains 1 (red) and 2 (blue).

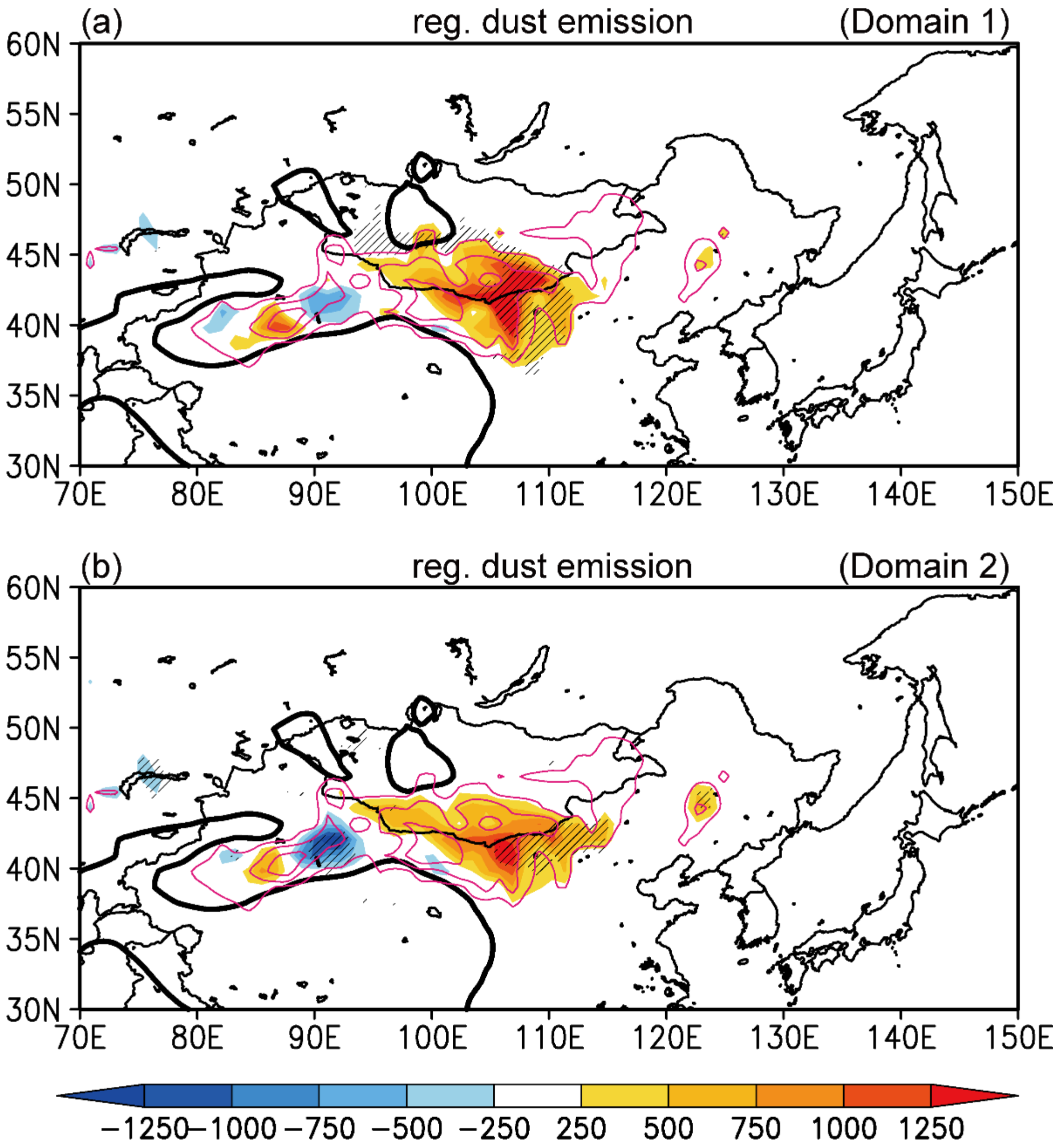

Fig. 2 Regression coefficients between the dust emission and dust deposition indices of Domains (a) 1 and (b) 2 in April (shading; unit: mg m^{-2} day^{-1}). The oblique lines denote where the correlation is significant at the 90% confidence level. The magenta contours indicate the mean dust emission from 2011 to 2017. The 500, 2000, and 4000 mg m^{-2} day^{-1} lines are plotted. The solid black contours indicate 2000 m topography.

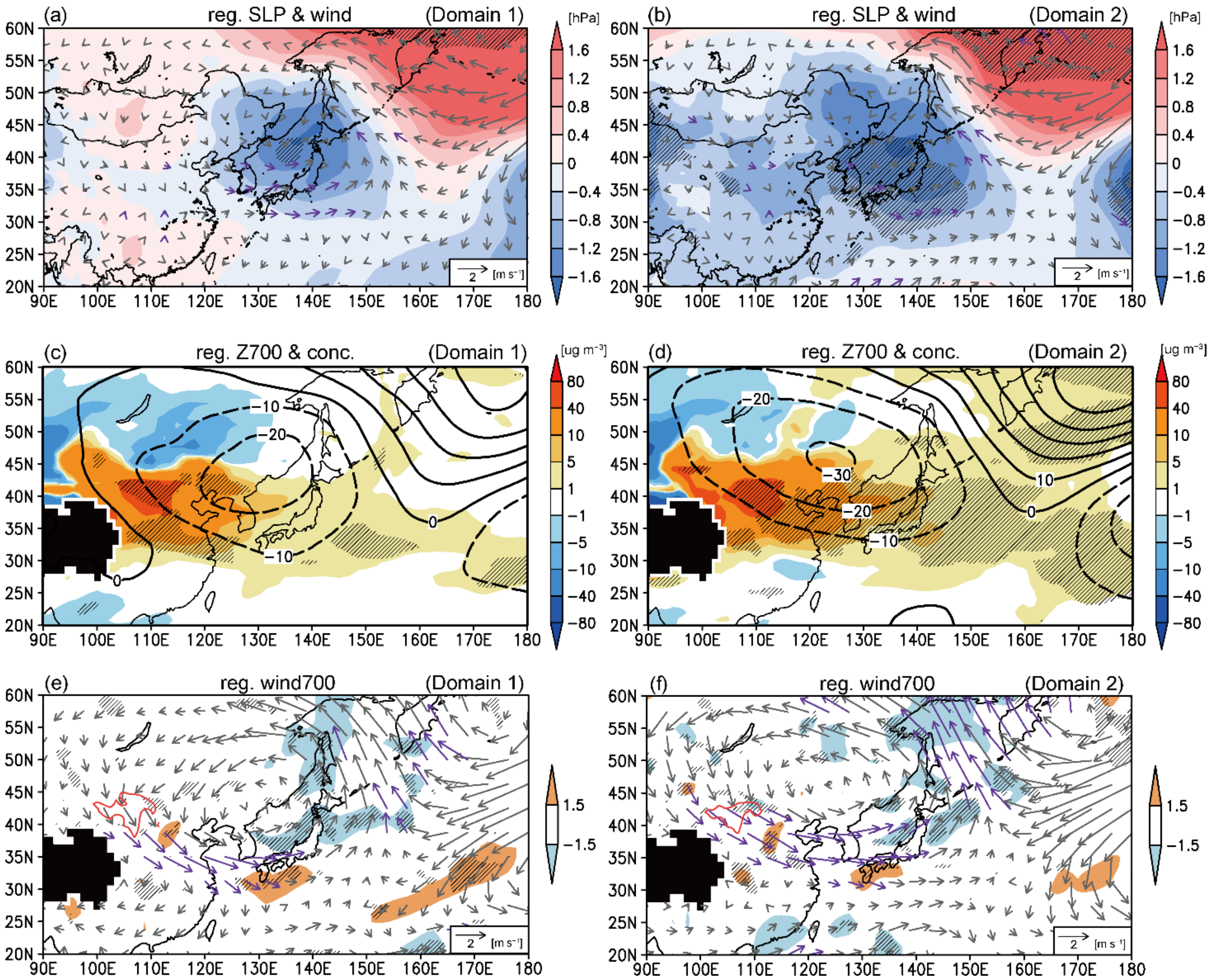

Fig. 3 Regression coefficients on the dust deposition indices of Domains (a, c, e) 1 and (b, d, f) 2 in April. (a, b) SLP (shading; unit: hPa) and surface winds 10 m above the ground (vector; unit: m s^{-1}). (c, d) Dust concentration (shading; unit: μg m^{-3}) and geopotential height (contours; unit: m) at 700 hPa. (e, f) Horizontal winds (vector; unit: m s^{-1}) and vertical p velocity (shading; unit: 10^{-2} Pa s^{-1}) at 700 hPa. In (e, f), the 750 mg m^{-2} day^{-1} lines of the regressed anomaly of dust emission (as the shading in Fig. 2) are superimposed by red contours. The oblique lines denote where the correlation between the shading variables and the indices is significant at the 90% confidence level. The purple vectors indicate where the zonal or meridional component is statistically significant at the

90% confidence level. The data below the local surface are masked.

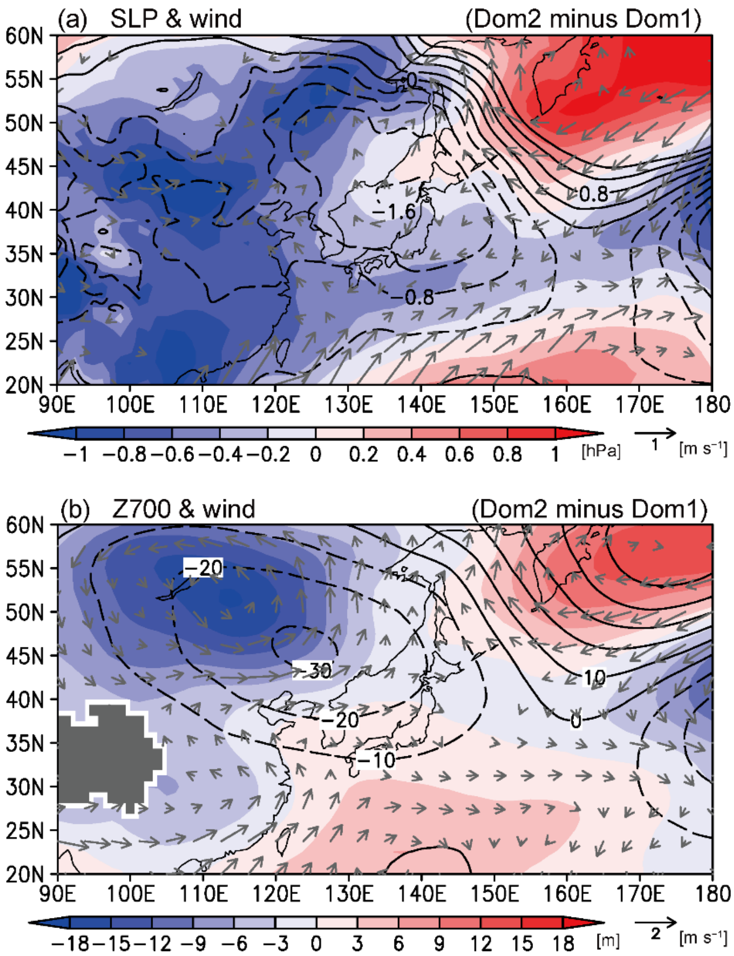

Fig. 4 Difference between the regressed anomalies associated with the dust deposition variations in Domains 1 and 2 (Domain 2 minus Domain 1 is shown) in April. (a) SLP (shading; unit: hPa) and surface winds 10 m above the ground (vectors; unit: m s^{-1}). Vectors below 0.1 m s^{-1} were omitted. (b) Geopotential height (shading; unit: m) and horizontal wind (vectors; unit: m s^{-1}) at 700 hPa. Vectors below 0.2 m s^{-1} were omitted. Contours in (a) and (b) represent the regressed anomalies of SLP and 700-hPa geopotential height for Domain 2, the same as the shading in Fig. 3b and contours in Fig. 3d, respectively.

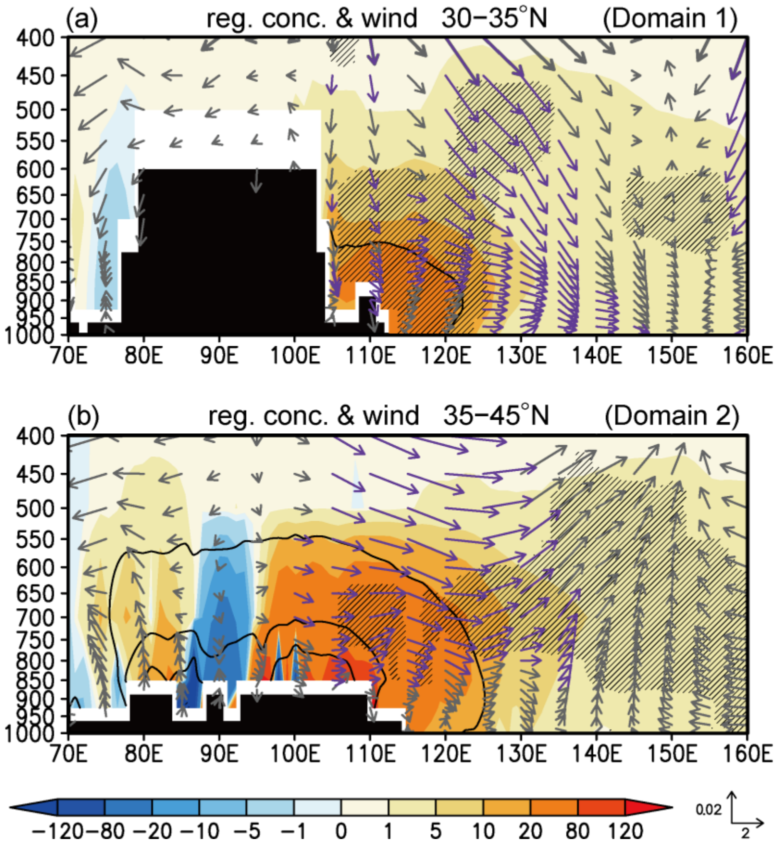

Fig. 5 Longitude–pressure cross-sections of the regression coefficients (a) along 30–35°N on the dust deposition index of Domain 1 and (b) along 35–45°N on that of Domain 2. The dust concentration (shading; unit: μg m^{-3}) and winds (vector; vertical unit: Pa s^{-1}; zonal unit: m s^{-1}) are plotted. The oblique lines denote where the correlation between the shading variable and the indices is significant at the 90% confidence level. The purple vectors indicate where the zonal or vertical component is statistically significant at the 90% confidence level. The thin black contours denote the April mean dust concentrations of 50, 200, and 400 μg m^{-3}. The data below the local surface are masked.

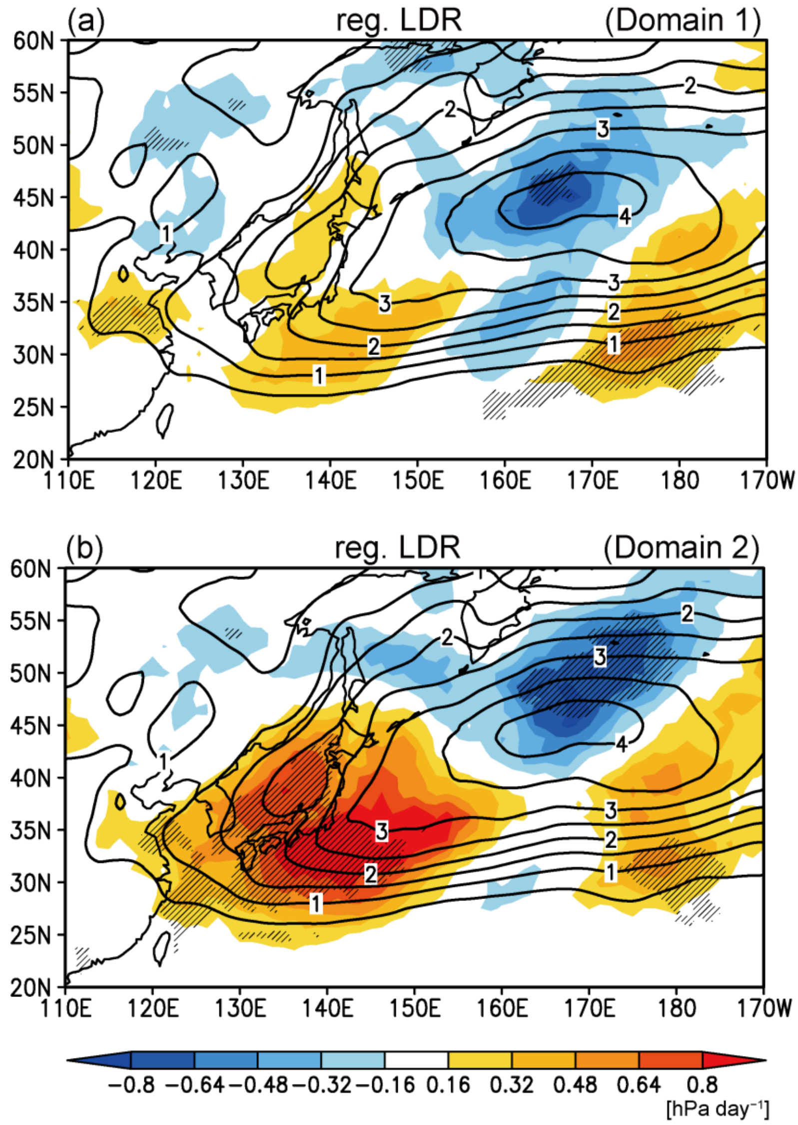

Fig. 6 Regression coefficients between LDR24P0.5 and the dust deposition indices of Domains (a) 1 and (b) 2 (shading). The oblique lines denote where the correlation is significant at the 90% confidence level. The black contours denote the mean LDR24P0.5 in April from 2011 to 2017. The units are hPa day^{-1}.

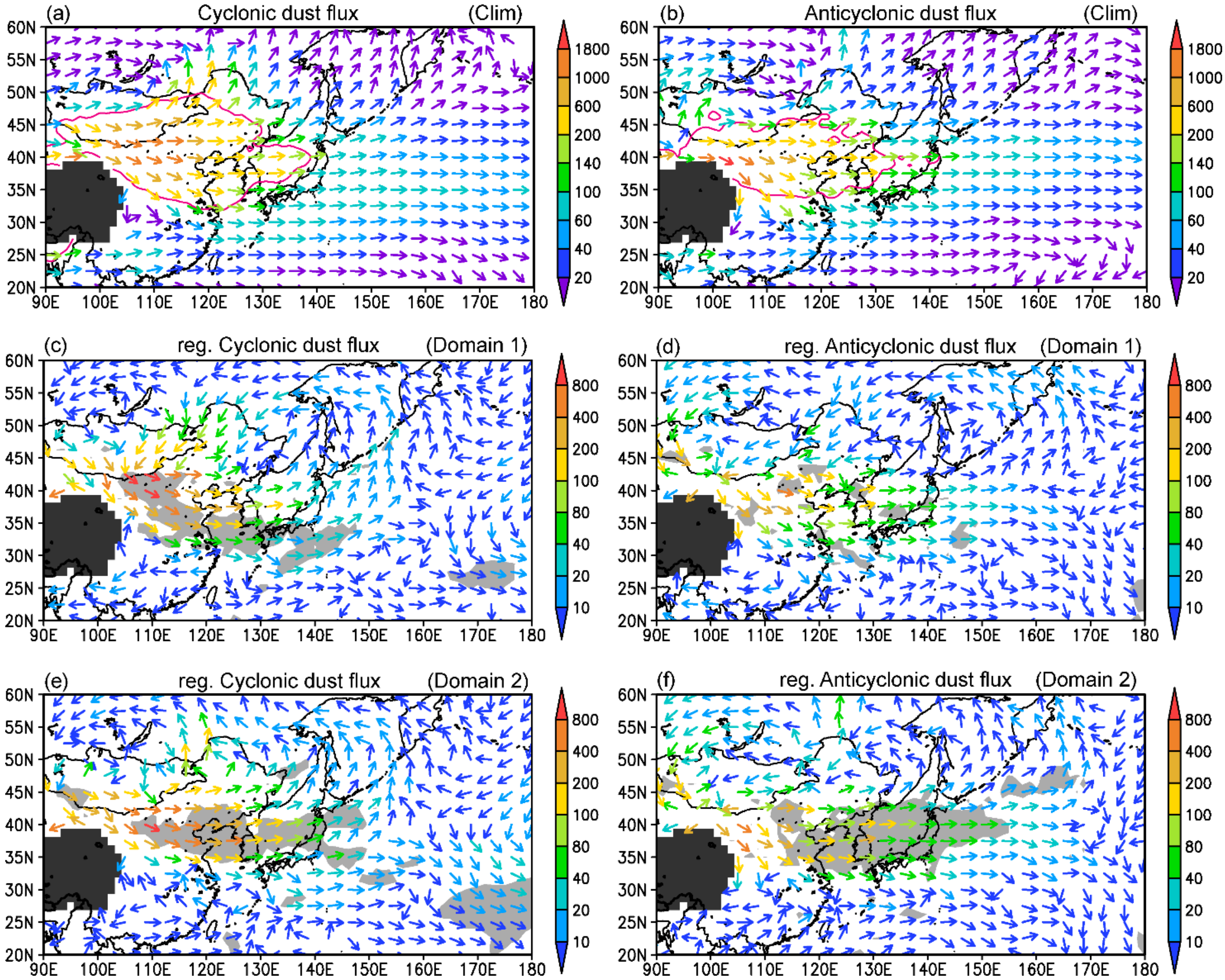

Fig. 7 (a, b) Mean cyclonic and anticyclonic dust fluxes at 700 hPa in April from 2011 to 2017, respectively (vector). The magenta contours indicate their zonal component of 140 μg m^{-2} s^{-1}. (c)–(f) Regression coefficients between the dust fluxes and dust deposition indices of Domains (c, d) 1 and (e, f) 2 (vector). (c, e) Cyclonic and (d, f) anticyclonic dust fluxes are displayed. The gray shading denotes where the correlation between the zonal components and indices is significant at the 90% confidence level. The magnitude of fluxes is indicated by colors and all units are in μg m^{-2} s^{-1}.

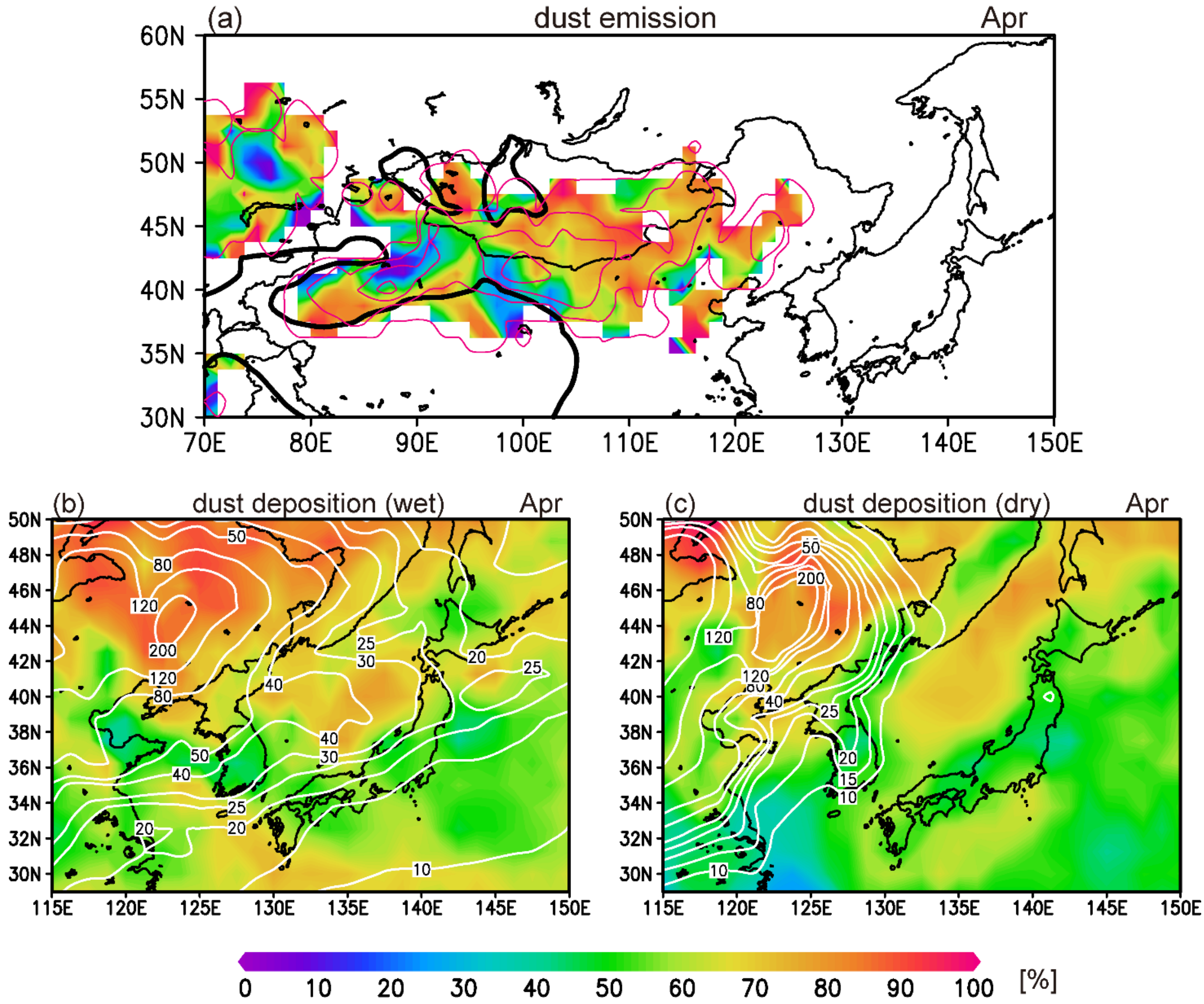

Fig. 8 Proportion of the cyclonic vortex contribution during April. (a) Cyclonic contribution to the mean dust emission (shading). The magenta contours indicate the mean dust emission from 2011 to 2017 of 5, 500, 2000, and 4000 mg m^{-2} day^{-1}. The solid black contours indicate 2000 m topography. (b, c) Cyclonic contribution to the mean wet and dry dust depositions, respectively (shading). The white contours indicate the mean dust deposition from 2011 to 2017 (unit: mg m^{-2} day^{-1}).

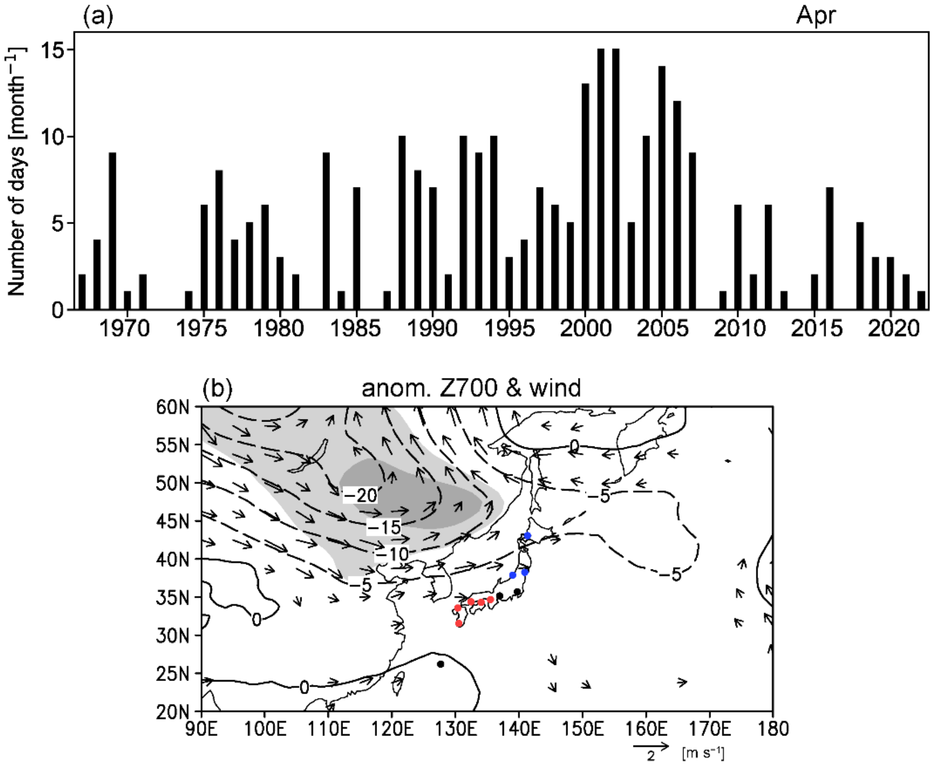

Fig. 9 (a) Interannual time series of the number of days in April that dust was observed at any observation station in Japan from 1967 to 2022. (b) Composited anomalies in April of geopotential height (contours; unit: m) and winds (vector; unit: m s^{-1}) at 700 hPa in the dust frequent years (the top 20%; 1969, 1983, 1988, 1992, 1993, 1994, 2000, 2001, 2002, 2004, 2005, 2006, and 2007). The anomalies are deviations from the climatological mean defined as a 30-year average from 1991 to 2020. Light and heavy shading indicate where the anomalies of geopotential height are significant at the 95% and 99% confidence levels, respectively. Vectors below 0.5 m s^{-1} were omitted. Color dots are plotted at the location of the 11 observation stations of JMA; red: western Japan (Osaka, Hiroshima, Takamatsu, Fukuoka, and Kagoshima; corresponding to Domain 1), blue: northern Japan (Sapporo, Sendai, and Niigata; corresponding to Domain 2), black: neither western nor northern Japan (Tokyo, Nagoya, and Naha).